Chapter 2
Optimization of the Fluidic Component of Complete Fluidic Sprinkler and Testing of the New Design Sprinkler

Abstract A newly designed dynamic fluidic sprinkler was developed to improve hydraulic performance of the existing complete fluidic sprinkler under low-pressure conditions. This study presents the orthogonal test of the newly designed dynamic fluidic sprinkler with different types of nozzles at different operating pressures. The following conclusions were made: These experiments confirmed the optimal values of the dynamic fluidic sprinkler structural parameters.

2.1 Introduction

Sprinkler irrigation technology has been widely used especially in agriculture to save water. It has great potential for improving the water use efficiency of crops. Furthermore, the irrigation engineer can control the amount of water applied, and it is more easily scheduled, which can increase water productivity per the unit of water consumed [1, 2]. The sprinkler irrigation system distributes water in the form of discrete drops travelling through the air [3]. Sprinkler irrigation can play a significant role in irrigation development in third world countries, if the system is properly selected, designed and operated. Sprinkler systems have accelerated and been revolutionized with the development of irrigated agriculture in several parts of the world. It is therefore not surprising that the utilization of sprinkler irrigation systems has recently increased [4, 5].

According to [6, 7], the performance of a sprinkler is determined by its discharge, wetted radius, distribution pattern, application rate and droplet sizes. Water application rate can be defined as the depth of water applied to the area per unit time. It determines which sprinkler should be assigned to a particular soil, crop and terrain on which it operates. The application rate depends on the operating pressures, the nozzle size and distance between sprinklers [8]. However, the effect of operating pressure on application rate is minimal compared to the effect of the sprinkler nozzle on the application rate [3]. For most sprinklers, when the operating pressure is increased, the discharge tends to balance the increase in wetted area. It has been found that a

sprinkler nozzle that produces little droplets covers a smaller wetted area, which also has the highest average application rate. Increasing the nozzle diameter increases the average application rate, since the sprinkler discharge tends to increase more rapidly than wetted area [9]. According to [10, 11], the application uniformity of a sprinkler is an important performance criterion for the design and evaluation of sprinklers, which is primarily influenced by operating pressure, sprinkler size and spacing.

Several studies have been conducted to analyze the droplet size distribution with different types of sprinklers over the years. The work in [12] showed that drop size distributions have a direct effect on irrigation water kinetics energy and wind drift. The work in [13] analyzed the droplet size characteristics of a complete fluidic sprinkle and concluded that about 50% of the droplets had a diameter of less 0.5 mm and that 50% of the water volume consisted of droplets with a diameter less than 2 mm at most distances. The work in [14] reported that nozzle size and pressure configurations have an influence on droplet formation. Similarly, [15, 16] reported that drop sizes can also influence the design, uniformity and efficiency of irrigation systems. According to [17], wind speed has been found to affect fine drops more than large drops. The work in [18] showed that small drops are subject to large evaporation losses under high vapor pressure. However, when drop evaporation is controlled by air friction, large drops can account for most evaporation losses [19]. The work in [20] reported that drops produced by a sprinkler are subject to several factors; such as the type of sprinkler and nozzle, operating parameters and environmental conditions.

Other researchers have proposed equations to express the coefficient of uniformity [21, 22]. The different equations available to express the coefficient of uniformity (CU) are based on some measures of variation in water distribution. The work in [23, 24] considered a coefficient of uniformity value of less than 85% as "low" and a CU of 85% or above as "desirable". According to [25, 26], Christiansen's coefficient of uniformity is the most widely used for water distribution uniformity assessment in sprinkler irrigation.

Over the years, extensive research works have been carried out to improve the structure and efficiency of the fluidic sprinkler for crop production. The work in [27] conducted experiments on drop size distributions and droplet characterization of a complete fluidic sprinkler with different nozzle dimensions. The work in [28] performed a numerical simulation and experimental study on a new type of variable-rate fluidic sprinkler. The work in [29] researched the field performance characteristics of a fluidic sprinkler. The work in [30] compared fluidic and impact sprinklers based on hydraulic performance. The work in [31] analyzed smoothed particle hydrodynamics and its applications in fluid–structure interactions. The work in [32] concluded that variations in quadrant completion times were small for both fluidic and impact sprinklers. However, deviations in water application rate were higher with the fluidic sprinkler. The work in [29] studied the relationship between rotation speed and operating pressure and pointed out that the inner angle of a fluidic sprinkler varied in quite a range among geometrical parameters. Subsequently, the authors concluded that further study needed to be carried out on the design features of the fluidic component. Similarly, Liu et al. [28] carried out a study on the fluidic sprinkler and confirmed the need to optimize the structure.

Only a few studies have focused on improving the rotation of the fluidic sprinkler. However, the rotation instability remains a major difficulty, resulting in the variation of the water application rates. Optimization can enhance the rotation stability and minimize the inconsistency in the water application rates. Therefore, the aim of this paper was to evaluate the hydraulic performance of the newly designed dynamic fluidic sprinkler with different types of nozzles at different operating pressures.

2.2 Complete Fluidic and Outside Signal Sprinklers

Figure 2.1a and b, show the schematic diagram of complete fluidic and outside signal sprinklers, respectively. In the figures, the main differences between the outside signal and a complete fluidic sprinkler are the working principle. The outside signal receives a signal when the jet flows impact on the signal device, located outside of the nozzle in the flow direction. But the complete fluidic sprinkler obtains a signal from the fluidic component, found in the inside of the working area. In previous studies, the authors made efforts to improve the performance of the fluidic sprinkler. However, the rotation instability remains a major difficulty, resulting in variations of the water application rates. Therefore, it is necessary to redesign the fluidic structure of the fluidic sprinkler by considering the contraction angle, the shape, and the size of the signal air hole. The aforementioned parameters used by previous are shown in Table 2.1.
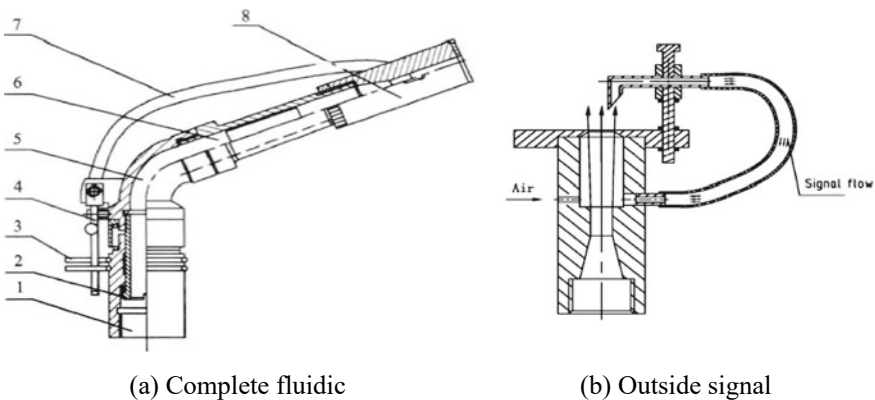

(a) Complete fluidic   (b) Outside signal

Fig. 2.1 Complete fluidic and outside signal sprinklers. 1. Swivel connection block; 2. Hollow shaft; 3. Limiting ring; 4. Reverse mechanism; 5. Signals water into faucets; 6. Sprinkler tubing; 7. Reversing plastic tube; 8. Fluidic element

**Table 2.1** Design parameters for outside signal and complete fluidic sprinklers

Parameter	Dimension	
	Outside signal	Complete fluidic
Contraction angle (α)	10º	20º
Diameter of base hole *(M)*	20 mm	8 mm
Offset length *(S)*	2.4 mm	2.8 mm
Working area *(L)*	43 mm	28 mm

2.3 Design of Newly Dynamic Fluidic Sprinkler Head and Working Principle

2.3.1 Working Principle

Figure 2.2 presents the structure of dynamic fluidic sprinkler. The profile of the fluidic element was defined by the inner contraction angles, the offset length, and the working area. A prototype of the dynamic fluidic sprinkler was self-designed and locally machined by using a wire-cut electric discharge machining process. The manufacturing tolerance for the size was ±0.02 mm as shown in Fig. 2.2. The working theory of (DFS) is based on the theory of the Coanda effect. The dynamic fluidic sprinkler receives an air signal from a signal tank. The working principle of the fluidic sprinkler is as follows: as water is ejected from the nozzle of the main tube into the signal thank, a region of low-pressure forms on both sides at the entry into the main jet flow. Fluid flow from the reversing plastic tubing (left) into the right side, forces the jet to deflect towards the right boundary of the signal thank where it eventually attaches. The air gap between the exit at the right side of the element and the water jet is filled by air, such that the pressures on both sides of the main jet are equal. At the same time, the nozzle receives the signal water on the left edge of the water jet, then the signal water flows in the tube to the inlet signal. Taking out the water from the contact signal into the inlet, the small gap is eventually blocked, forming a low-pressure region. When the pressure difference reaches a certain value, the main jet flows to the right-side attachment wall, Water flows from the diameter into the action zone, and the main jet is ejected from the central circular hole. Under the wall attached condition, due to the bending of the main jet, the signal water nozzle is void and no signal water is received, only air is received. After the signal water in the tube is pumped out, the air enters the water inlet through the tube. The pressures on both sides become equal. Alternate air movement from the signal nozzles and the plate cover account for the stepwise rotation [32].

Fig. 2.2 Schematic, pictorial view of the newly fluidic sprinkler head. 1. Water signal tank. 2. First, lock nut. 3. Pipe sprayer 4. Spray body. 5. Second lock nut. 6. Body of the fluidic element. 7. Jet element body. 8. Water inlet. 9. Air hole. 10. Outlet cover plate. 11. Water dividing hole. 12. α degree. 13. Signal nozzle. 14. Third lock nut. 15. Conduit
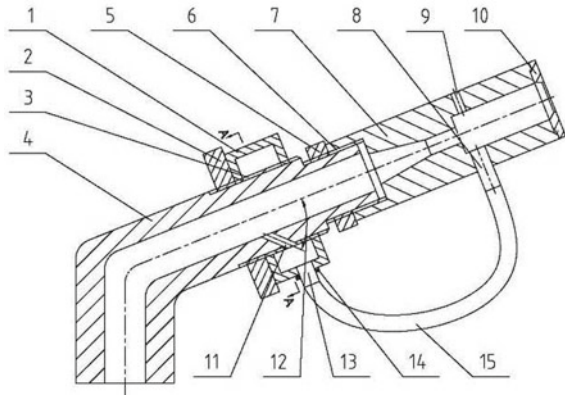
2.3.2 Design of the Nozzles

The equipment and design factors in the sprinkler irrigation system include the nozzle characteristics which are composed of nozzle size, nozzle type, discharge angle, jet straightening vane inside the main nozzle, the number of nozzles and operating pressure. Most sprinklers have two nozzles, the main nozzle and an auxiliary nozzle that discharge water in the form of a jet into the air. Nozzles convert the pressure within the piping system into velocity upon exist from the sprinkler. The wetted coverage area and the application pattern are determined by the nozzle design and the type of sprinkler. Other researchers have studied the influence and measurement of nozzle shape on sprinkler droplet size and water application. Several types of nozzles have been developed for fluidic sprinkler including constant- diameter, and diffuse-jet. Table 2.2 presents nozzles size and corresponding pressures for the previous study, looking at the increasing cost of energy and the growing demand to saving water for optimum crop production, it is more convenient to design new nozzles size for the study. Therefore, the test nozzles were self-designed and locally machined using a wire-cut electric discharge machining (EDM) process. The prototypes of the nozzles are shown in Fig. 2.3. The inlet diameter of the nozzle was set as 15 mm, while the outlet diameters were chosen as 3, 4, 5, 6, and 7 mm.

Table 2.2 Nozzles size and corresponding pressures for the previous study

Sprinkler type	Nozzle diameter (mm)	Pressure/kPa
10PXH	4	250
15PXH	6	300
20PXH	8	350
30PXH	10	400
40PXH	14	450
50PXH	18	500

(a) DFS sprinkler head   (b) Plate cover

Fig. 2.3 Prototype of the dynamic fluidic sprinkler and nozzle sizes

Table 2.3 Factors and levels

Level	Factors			
	A length of tube, l (mm)	B Pressure h, (mm)	C diameter of tube, m (mm)	D Nozzle diameter, n (mm)
1	15	150	2	5
2	20	200	3	6
3	25	250	4	7

2.3.3   Experimental Setup and Procedure

The hydraulic performances of structural parameters of the dynamic fluidic sprinkler were studied using an orthogonal test to determine influencing factors, the order of importance and optimal combination of the factors. The structural parameters of the sprinkler used for the study were the length of the tube (L), pressure (H), the diameter of the tube (M), nozzle diameter (N), and are represented by Factors A, B, C, and D, respectively. An orthogonal array with four factors and three levels was selected for the test as shown in Table 2.3. The tests were conducted in the sprinkler laboratory of the Research Center of Fluid Machinery Technology and Engineering, Jiangsu University in China. The laboratory is circular-shaped with a diameter of 44 m. The materials used for the experiment include; centrifugal pump, electromagnetic flow meter, and piezometer, valve and the impact sprinkler. The sprinkler was installed at a height of 2 m from the ground level with nozzle an elevation angle of 23°. The riser was at an angle of 90° to the horizontal from which the top of the catch cans was 0.9 m above the ground. Water was pumped from the reservoir through the main pipe and sprayed out from the nozzle. The working pressure was measured by a pressure gauge at the base of the sprinkler had an accuracy of 0.4%. The sprinkler was run for 30 min to standardize the environment conditions before the experiment

Table 2.4 Scheme used in the orthogonal test

Test	A	B	C	D
1	1	1	1	1
2	1	2	2	2
3	1	3	3	3
4	2	1	2	3
5	2	2	3	1
6	2	3	1	2
7	3	1	3	2
8	3	2	1	3
9	3	3	2	1

was carried out. Different inlet pressures were tested during the investigation and these include 150, 200 and 250 kPa. The corresponding flow rate was 1.47, 1.57 and 1.66 m^3/h for 150, 200 and 250, respectively. ASAE approach was used to determine the application of water depth measurements. The catch cans were used to collect water in an hourly base and measured with a graduated cylinder (Table 2.4).

The discharge coefficients of each nozzle were determined for the observed pressure-discharge data using Eq. (1.1).

Matrix Laboratory (MATLAB) program was used to compute the combined CU values according to the radial water distribution. Radial data of water distribution from the fixed water dispersion devices were modified into net data. The final calculated average radial water distribution data was the same in all directions from the A1, B1, C1, A2, B2, and C2. The available data points were distributed like a spider web. A grid of data points was converted to calculate the combined CU. The depth of the net point depends on the distance away from the sprinkler. The water depth of every interpolating point, assumed to be a continuous variable value, were calculated using a mathematical model of interpolating cubic splines. The uniformity of water application rate was evaluated using the Christiansen coefficient of uniformity (CU) in Eq. (1.5).

The direct analysis technique was used to analyze our test results. This technique can identify influencing factors in decreasing order of importance, and the optimal combination of factors can be forecasted. The calculation formula is as follow:

Y1X (Y2X, Y3Z) = Sum of corresponding data 1(2, 3) for

$$\text{Column} X \ j \ (X = \text{A, B, C, D}; \ j = 1, 2, 3) \tag{2.1}$$

$$\text{YIX (Y2X, Y3X)} = \text{Average of Y1X (Y2X, Y3X)} \tag{2.2}$$

$$\text{RX} = \text{Maximal YJX minus the minimal YJX} \tag{2.3}$$

Table 2.5 Discharge coefficient for different types of nozzles

Nozzle size (mm)	Pressure (kPa)	Discharge			
		150	200	250	Standard deviation
5		0.75	0.77	0.79	0.0163
6		0.85	0.76	0.66	0.077
7		0.70	0.56	0.59	0.060

2.3.4   Results and Analysis of Orthogonal Tests

2.3.4.1   Comparison of Operating Pressure and Discharge

Table 2.5 presents the results of measured flow rates of sprinkler irrigation nozzles used in this study under different operating pressures. Analysis of the measured data was performed to find the influence of the geometrical parameters as well as the operating pressure on the discharge of the sprinkler. As shown in Table 2.5, when using the sprinkler, the measured nozzle flow rates ranged from 1.4to 1.47 m³/h with a mean value of 1.435, 1.5 to 1.57 m³/h with a mean value of 1.535, and 1.59 to 1.66 m³/h with a mean value of 1.625, for 150, 200 and 250 kPa, respectively. The coefficient of discharge for 5 mm nozzle ranged from 0.75 ~ 0.79 with an average value of 0.77, while that from the 6 and 7 mm was from 0.66 ~ 0.85, 0.56 ~ 0.59 with an average of 0.756 and 0.62, respectively. From the analysis, it was established that the coefficients of discharge fluctuated within a small acceptable range under the same operating pressures. The coefficients of discharge obtained using 4 mm nozzle were higher than those obtained using the 5 and 6 mm nozzles, which means that the 4 mm nozzle had the advantages of higher irrigation intensities. These can be attributed to fewer restrictions within the inner flow movement. It can be confirmed that the discharge coefficient does not depend on the operating pressure. Similar results were published by.

2.3.4.2   Summary Results of the Orthogonal Test

Tables 2.6 and 2.7 and present the results of factors influencing the CUs and the spray range. From the study, the relatively ideal results should be higher uniformity coefficient and spray range. It was revealed that test 2 (A1 B1 C1 DI), test 6 (A2 B3 C1 D2), and test 7 (A3 B1 C3 D2), had the highest uniformity coefficient. This could be attributed to the fact that flow rate at same pressure was much higher and turbulence flow was less uniform resulting in better distribution. Test 1 (A1 B1 C1 DD1), test 2 (A1 A2 C2 A2), and test 7 (A3 B1 C3 D2) also had the highest spray range. Test 3 (A1 B3 C3 D3), test 4 (A2 B1 C2 D3) and test (A2 B2 C3 D1) were normal. Test 8 (A3 B2 C1 D3), and test 9 (A3 B3 C2 D1) were not effective because low uniformity and spray range were observed. As shown in Table 2.6, a higher R-value shows that the factor had a strong effect on the test results, which means that

Table 2.6   Test scheme and results

Test number	A	B	C	D	CU (%)	Range(m)
1	1	1	1	1	85	12
2	1	2	2	2	86.5	12
3	1	3	3	3	85.5	8
4	2	1	2	3	85.5	8
5	2	2	3	1	83.9	11
6	2	3	1	2	86	8
7	3	1	3	2	91	13
8	3	2	1	3	85	7
9	3	3	2	1	83.4	9

Table 2.7   Results of structural parameter combination

		A	B	C	D
CU	Yj1	240.00	242.50	241.20	236.35
	Yj2	239.60	239.40	240.45	244.70
	Yj3	240.45	140.15	240.40	241.00
	Yj1	80.67	80.83	80.40	78.78
	Yj2	79.87	79.80	80.15	81.57
	Yj3	80.15	80.05	80.13	80.33
	R	0.80	1.03	0.27	2.78
Range	Yj1	31.00	31.00	27.00	32.00
	Yj2	25.00	29.00	26.00	32.00
	Yj3	29.00	35.00	22.00	32.00
	Yj1	10.30	10.30	9.00	10.67
	Yj2	8.33	9.67	8.67	10.67
	Yj3	9.67	10.33	10.67	7.00
	R	2.00	2.00	2.00	3.67

the factor is significant, a lower R-value indicates that the factor had a weak effect on the test results, which means that it is not significant. The following observations can be drawn from the results shown in Table 2.6 and Fig. 2.4.

Factor A: When the length of the tube was varied from 20 to 25 mm, the CUs varied from 85% to 86.5% with an average value of 85.6 (A = 15 mm), from 83.9% to 87% with an average of 85.3 (A = 20), and from 83.4% to 91% with an average of 86.46% (A = 25 mm). The range also varied from 8 to 12 m with an average of 10.3 m (A = 15 mm), from 6 mm to12mm with an average of 8.3 m (A = 20 mm), and from 7 to 13 mm with an average of 9.6 m (A = 25 mm). The sprinkler worked perfectively at a length of 25 mm, but when the nozzle was 6 mm regardless of
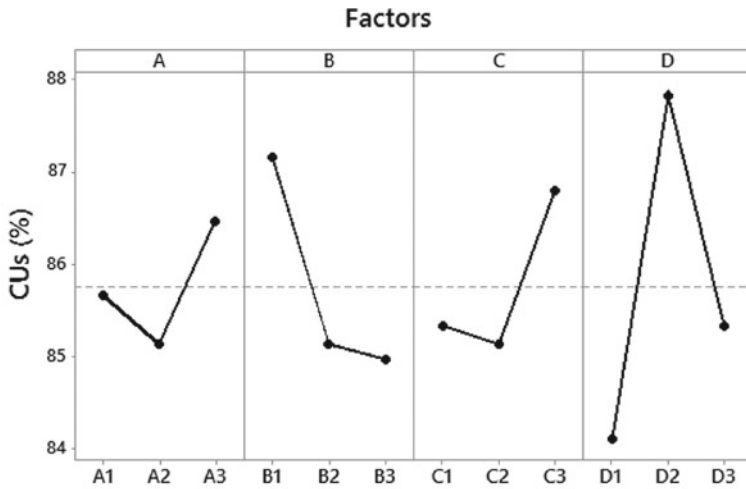
(a) Relationship between CU and the factors
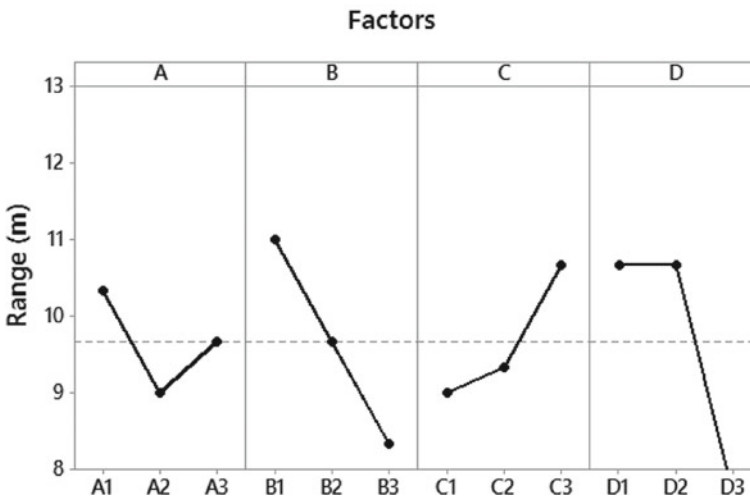
(b) Relationship between Range and the factors

Fig. 2.4 Factors influencing CUs and range

structure parameter changes, the sprinkler was not effective when the length of the tube was less than 20 mm or greater than 25 mm.

Factor B: When operating pressure was varied from150 to 250 kPa, the CUs increased from 85 to 91% with an average of 87.16% (B = 150 kPa), from 85.5% to 86.5% with an average of 85.7% (B = 200 kPa), and from 83.2% to 86.2% with an average of 84.9% (B = 250 kPa). The spray range varied from 6 to 13 m with

an average of 10.3 m (B = 150 kPa), from 7 to 11 m with an average of 8 m (B = 200 kPa), and from 8 to 9 m with an average value of 8.33 m (B = 250 kPa). The CUs and spray were significantly reduced with increasing working pressure. These can be attributed to restriction of the flow of water within the sprinkler resulting in a low amount of water application.

Factor C: When the diameter of the tube was varied from 2 to 4 mm, the CUs changed from 85 to 87% with an average of 85.66% (C = 2 mm), from 83.4% 86.5% with an average of 85.0% (C = 3 mm), and from 83.91% to 91% with an average of 86.8% (C = 4 mm). The spray range varied from 7 to 12 m with an average of 9 m (C = 2 mm), from 6 m to11m with an average of 8.67 m (C = 3), and from 8 to 13 m with an average of 10.7 m (C = 4 mm). The CU was highest at 3 mm because the overlaps were higher and the water distribution was more uniform when the tube was narrow.

Factor D: The nozzle diameter was varied from 4 to 6 mm. The CUs changed from 83.9% to 85% with an average of 84.1% (D = 4 mm), from 86.5% to 91% with an average value of 88.16% (D = 5 mm), and from 80% to 80.5% with an average value of (D = 6 mm). The range varied from 9 to 12 m with an average of 10.66 m (D = 4 mm), from 11 to 13 m with an average of 10.7 m (D = 5 mm), and from 6 to 8 m with an average of 7 m (D = 6 mm). The CUs and spray range decreased as the diameter of the nozzle was increased because a larger part of the jet flow was uninterrupted particularly in the case of the nozzles with the diameters of 6 mm. The optimal nozzle diameter was found to be 5 mm. The comparison of the test scheme indicated that CUs exceeded 85% in 5 tests, and the range exceeded 10 m in 4 tests. Tests 7 and 2 were ideal. Test 7 (A1B1C1D2) had the highest uniformity coefficient and the longest range. Test 5 was not effective because B was too small when D was a lager. Test 9 was also ineffective because B was too large when D was small. The optimal combination of structural parameters was achieved with the factor combination of A3B1C3D1.

2.3.4.3   Simulation of Water Distribution

Figure 2.5 presents the plots of water distribution for all the 9 tests. It can be observed that variations in the contour and color maps around the sprinkler had different application rates. Rings that have similar color indicate uniform water distribution pattern, whiles different colors in the ring represent non-uniform water distribution patterns.

Comparison of water distribution for the various tests showed that test 7 and test 2 produced a high uniformity for a given operating pressure which corresponds to the orthogonal results. However, test 7 was slightly higher compared to test 2. It is possible that after interruption with the alignment signal nozzle the flow became less uniform, leaving more water applied near the sprinkler. This means that test 7 can improve the uneven distribution of water and save water for crop production. As a consequence, differences in water distribution can be seen in most areas around the sprinkler in the case of the other tests, which is in agreement with [33] reported
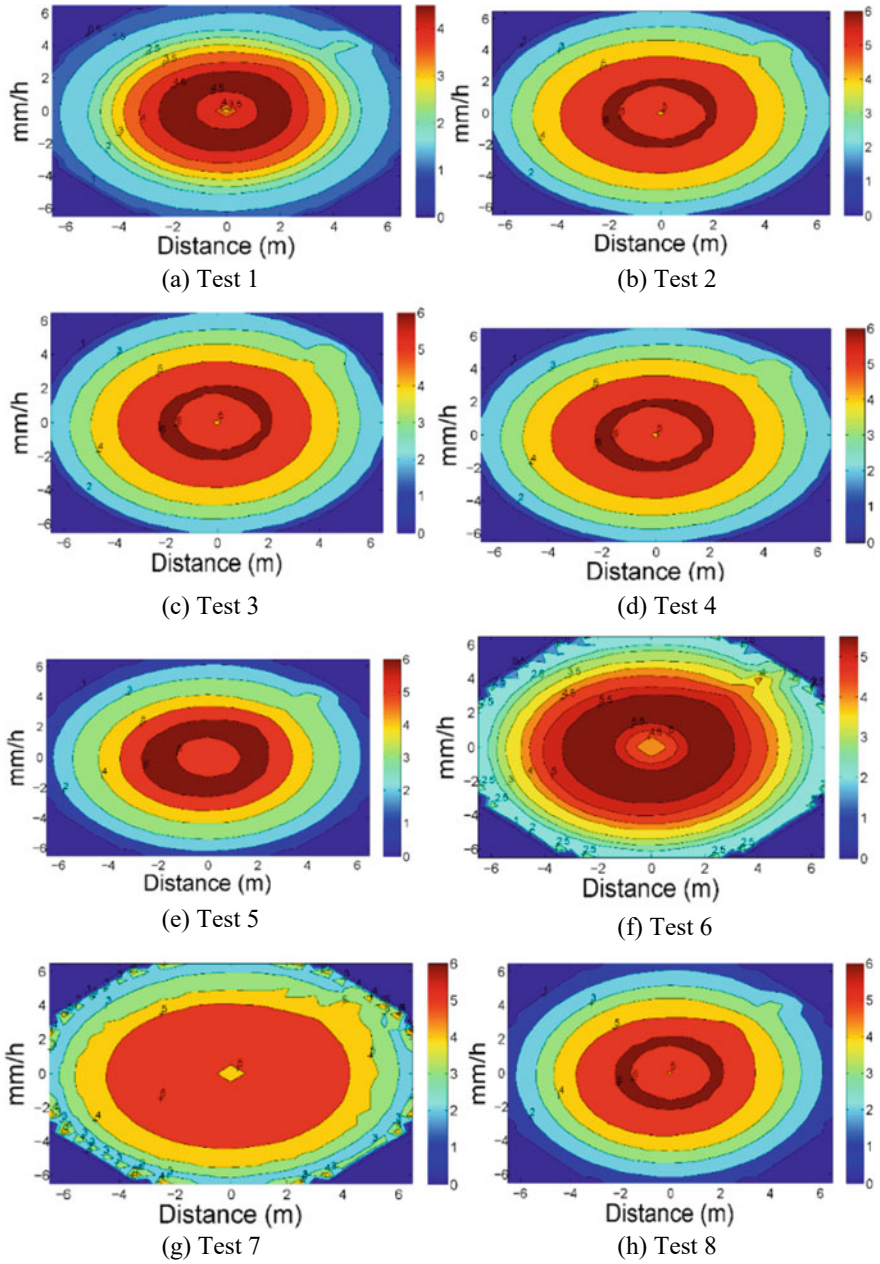
(a) Test 1

(b) Test 2

(c) Test 3

(d) Test 4

(e) Test 5

(f) Test 6

(g) Test 7

(h) Test 8

Fig. 2.5 An illustrative example of water distribution maps for tests 1 through 9
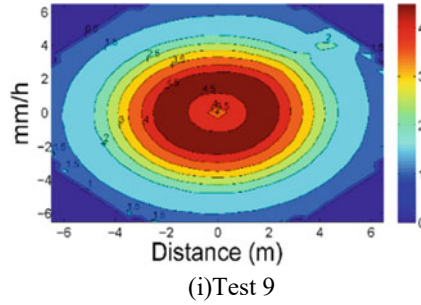
(i)Test 9

Fig. 2.5 (continued)

similar results in their experiments using fluidic sprinkler results of variations in rotations speed with respect to the quadrants.

2.3.5 Brief Summary

This study presents the orthogonal test of the newly designed dynamic fluidic sprinkler with different types of nozzles at different operating pressures. The following conclusions were made: These experiments confirmed the optimal values of the dynamic fluidic sprinkler structural parameters. The length of the tube is 25 mm, the working pressure is 150 kPa, the diameter of the length of the tube is 3 mm, and the nozzle diameter is 5 mm. The factors influencing the CU and range in decreasing order of importance were nozzle diameter, pressure, length of the tube and the diameter of the tube. The optimal combination of structural parameters was achieved with the factor combination of A3B1C3D1.

2.4 Evaluation of Hydraulic Performance Characteristics of a Newly Designed Dynamic Fluidic Sprinkler

2.4.1 Design of New Dynamic Fluidic Sprinkler Head

In this research, a newly designed dynamic fluidic sprinkler head was manufactured. The following parameters are key factors when it comes to the design of the fluidic structure: the diameter of the main nozzle, the inner contraction angle, the offset length and the working area. The dynamic fluidic sprinkler was developed by Jiangsu University. It is schematically shown in Fig. 2.6. The manufacturing tolerance for the size was ±0.02 mm. The main differences between the newly designed dynamic fluidic sprinkler (DFS) and complete fluidic sprinkler (CFS) is the working principle.
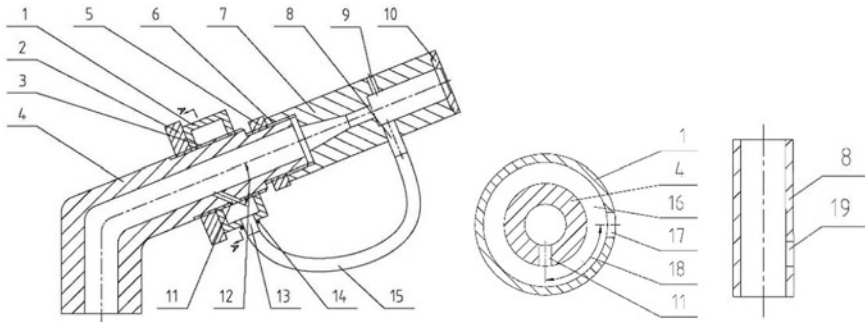
Fig. 2.6 Schematic, pictorial view of the new fluidic sprinkler head. 1. Water signal tank. 2. First lock nut. 3. Pipe sprayer 4. Spray body. 5. Second lock nut. 6. Body of the fluidic element. 7. Jet element body. 8. Water inlet. 9. First air hole. 10. Outlet cover plate. 11. Water dividing hole. 12. α main flow.13. Signal nozzle. 14. Third lock nut. 15. Conduit. 16. Water storage capacity. 17. Signal hole. 18. β contraction angle. 19. Second air hole

The newly designed dynamic fluidic sprinkler receives an air signal from a signal tank, but the complete fluidic sprinkler obtains the signal from the fluidic component, found in the working area. When they are operating under a low pressure condition (such as 100 kPa), it is difficult to get the signal flow for the complete fluidic sprinkler. This leads to disappearance of the pressure difference between the two sides of the wall. Therefore, the CFS rotation could not be guaranteed. For the DFS, the air signal flow could be received continuously once the signal tank is filled with water.

2.4.2 Working Principle

The principle of operation of the fluidic sprinkler is based on [34] to perform the function of rotation. Water is ejected from the main nozzle to the working area. A region of low-pressure eddy is formed on both sides of the working area. Air flows into the left side from the reverse blow down nozzle and into the right side from the signal nozzle. The main flow jet is straight because the pressure on both sides is equal and the sprinkler remains stationary, as shown in Fig. 2.7a,b, respectively. The signal flow received from Signal Nozzle 1 fills up Signal Nozzle 2 to transform the right side into a low-pressure eddy. The main flow jet is bent toward the boundary and eventually attached to it because the left pressure is much larger than the right pressure. The phenomenon is repeated step by step, and the sprinkler achieves a stepwise rotation in sequence by self-control. The main flow jet is reattached to the left plane, and the sprinkler rotates to the opposite direction because the right pressure is much larger than the left pressure. The reverse blow down nozzle opens, and air flows into the left side to equalize the pressure again when the sprinkler rotates to the other side.
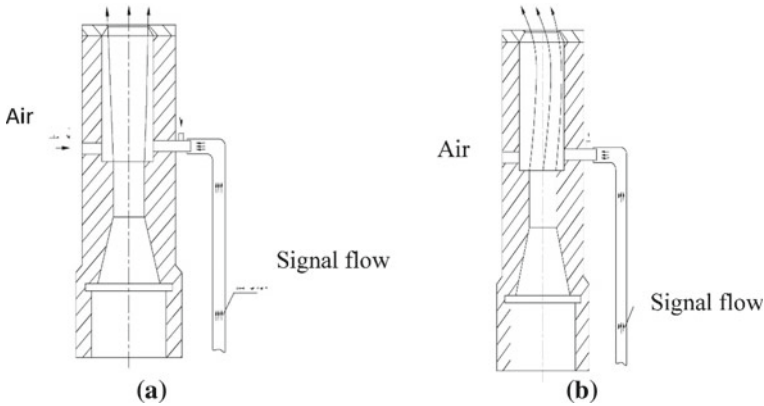
Fig. 2.7 a Straight main flow jet. **b** Main flow jet reattached to the right

2.4.3 Experimental Procedures

The experiments were conducted at the indoor facilities of the Research Center of Fluid Machinery Engineering and Technology, Jiangsu University (Jiangsu province). The diameter of the circular-shaped indoor laboratory was 44 m. A centrifugal pump was used to supply water from a constant level reservoir. The sprinkler head was mounted on a 1.5 m riser at a 90° angle to the horizontal. Catch cans used in performing the experiments were cylindrical in shape, 200 mm in diameter and 600 mm in height. The catch cans were arranged in two legs around the sprinkler as shown in Fig. 2.8. Each leg contained 14 catch cans placed 1 m apart constituting 28 catch cans in total. The sprinkler was run for some minutes to standardize the environment conditions before the experiment was carried out. The sprinkler flow rate was 4.75 m³/h for an operating pressure of 250 kPa, which was controlled by pressure regulation. The operating pressure at the base of the sprinkle head was regulated and maintained by a valve with the aid of a pressure gauge with an accuracy of ± 1%.The corresponding operating pressures were 100, 150, 200, 250 and 300 kPa, respectively. The application of water depth measurements was carried out in accordance with [31].

The experiment lasted for an hour, and the water depth in the catch cans was measured with a graduated measuring cylinder. Droplet sizes were determined using a Thies Clima Laser Precipitation Monitor (TCLPM). It has the following specification: the drop diameter measurement ranges from 0.125 to 8.5 mm in increments of 0.125 mm, and the measuring area is 228 mm long, 200 mm wide with a thickness of 0.75 mm, manufactured by Adolf Thies GMBH & CO. KG, Gottingen, Germany. The principle of operation is such that a beam of light is produced from a laser-optical source in the form of infrared, 785 nm. A photo-diode with a lens is located on the receiver side to determine the optical intensity after transformation into electrical signals. The receiving signal reduces when the water droplet falls through the

Fig. 2.8 Experimental setup in the indoor laboratory

measuring area. The diameter of the droplet is estimated from the amplitude of the reduction, the droplet velocity of which is calculated from the duration of the reduced signal. For each operating pressure, the droplet size distributions were determined at an interval of 2 m along a radial transect at a distance of 2 m from the sprinkler. For each droplet measurement, the sprinkler was allowed to rotate over the TCLPM at least five times to ensure a sufficient number of drops passed through the measured area. At each pressure, a minimum of three replication assessments were made, and the averaged data were used for the final experiments. Data were ordered according to the drop diameter.

2.4.4 Computed Coefficient of Uniformity

Matrix Laboratory (MATLAB R2014a) software manufactured by Mathwork Incoperation, Springfield, MA, USA was employed to establish a computational program for the CU. The work in [25, 26] reported that Christiansen's coefficient of uniformity is the most widely used and accepted uniformity criterion. Therefore Christiansen's equation was utilized to determine CU.

$$CU = \left(1 - \frac{\sum_{i=1}^{n}|X_i - \mu|}{\sum_{i=1}^{n}X_i}\right)100\% \tag{2.4}$$

where n = number of catch cans; x_i = measured application depth, mm; μ = mean average depth, mm; and CU = coefficient off uniformity, %.

The model for converting radial data into the net data's insert function was established as follows: Point A is the net point between two adjacent radial rays, and (X_k, Y_k) is its coordinate. P_1, P_2, P_3 and P_4 are the four nearest points to Point A on the adjacent radial rays, and $(P_1 Q_1)$, $(P_2 Q_2)$, $(P_3 Q_3)$ and $(P_4 Q_4)$ are their coordinates. Their positions are therefore $x_1 = P_1 \cos\varnothing_1$, , $(i = 1, 2, 3, 4)$ and $y_1 = P_1 \sin\varnothing_1$, $(i = 1, 2, 3, 4)$; their water depths are h_1, h_2, h_3 and h_4; and the distances away from Point A are r_1, r_2, r_3 and r_4, respectively. Thus,

$$r_1 = \sqrt{(Xi - Xk)^2 + (Yi - Yk)^2}(i = 1, 2, 3, 4) \tag{2.5}$$

The water depth A can be expressed as:

$$h_A = C_1 h_1 + C_2 h_2 + C_3 h_3 + C_4 h_4 \tag{2.6}$$

where:

$$C_1 = (r_2 r_3 r_4)^2/R, \; C_2 = (r_1 r_3 r_4)^2/R, \; C_3 = (r_1 r_2 r_4)^2/R, \; C_4 = (r_1 r_2 r_3)^2/R, \tag{2.7}$$

$$R = (r_1 r_2 r_3)^2 + (r_1 r_3 r_4)^2 + (r_1 r_2 r_4)^2 + (r_2 r_3 r_4)^2 \tag{2.8}$$

According to the actual measurements, the water depth of every point can be calculated using Eq. (2.5). The combined coefficient of uniformity can then be calculated for the overlapping of the spray sprinkler with different lateral spacings.

Basic drop statistics: Managing the large dataset obtained from the photographs required a statistical approach. While it is convenient to represent the sets by a reduced number of parameters, some traits of the drop populations can be obscured by the choice of statistical parameters. The parameters used in this work for drop diameter included arithmetic mean diameter (Eq. (2.9)), standard deviation (Eq. (2.11)) and coefficient of variation (Eq. (2.12)). The following addition parameters were determined for drop diameter: the volumetric mean (D_v) and average volumetric diameter (D_{50}).

$$\bar{d} = \frac{\sum_{i=1}^{n} m_i d_i}{\sum_{i=1}^{n} m_i} \tag{2.9}$$

$$d_v = \frac{\sum_{i=1}^{n} d_i^4}{\sum_{i=1}^{n} d_i^3} \tag{2.10}$$

$$SD_D = \sqrt{\frac{1}{n-1} \sum_{i=1}^{n} \left(d_i - \bar{d} \right)^2} \tag{2.11}$$

$$CV_D = \left(\frac{SD_D}{\bar{d}}\right) \times 100 \tag{2.12}$$

where d_i = the diameter of the droplet in each set (mm), n_i = the droplet number, i = the number of droplets in the set, $\bar{d}$ = the arithmetic mean droplet, d_v = the volume weighted average droplet diameter, SD_D = the standard deviation and CV_D = the coefficient of variation.

In order to test the difference between the means of the independent samples of 150 and 250 kPa, the study employed an independent sample t-test where variances were assumed to be equal with the t-test statistics formulated as:

$$t = \frac{\left(\overline{X}_1 - \overline{X}_2\right) - (\mu_1 - \mu_2)}{\sqrt{\frac{s_1^2}{n_1} + \frac{s_2^2}{n2}}} \tag{2.13}$$

where $\overline{x_1}$ and $\overline{x_2}$ are sample means, μ_1, μ_2 are population means, s_1^2 and s_2^2 are variances and n_1 and n_2 are the sample sizes for 150 and 250 kPa, respectively.

The above tests were carried out according to the standards of [35].

2.4.5 Results and Discussion

As shown in Table 2.8, the smallest radius of throw was obtained when the sprinkler was operated at the pressure of 100 kPa, and the maximum radius of throw was also obtained at 250 kPa for five of the six nozzles sizes tested in the present experiment. The difference between the maximum and the minimum radius of throw was 7.2 m. For all the nozzle sizes, the distance of throw increased with an increase in operating pressure until it reached 250 kPa, when it began to decrease. The distance of throw increased when the diameters of the nozzle sizes were increased, and it began to decrease for all the nozzle sizes. Similar findings were reported by [36]. This is possible because at a high pressure condition, the jet breaks up quickly, resulting in smaller radius of throw. For smaller diameters, the jet flow was restricted, resulting in a smaller radius of throw. The result from the independent sample t-test analysis (Table 2.9) showed that there was no significant different between radius of throw for 250 and 150 kPa since ($p > 0.05$). The obtained results for the radius of throw were similar to previous findings by Zhu et al. [32].

Table 2.8 Radius of throw for different types of nozzles and pressures

Nozzle size (mm)	Radius of throw (m)					Standard deviation (m)				
	p									
	100	150	200	250	300	100	150	200	250	300
2	6.4	7.4	7.9	8.7	8.1	0.2	0.3	0.5	0.3	0.7
3	8.5	9.7	10.7	11.7	10.7	1.2	0.1	0.6	0.2	0.4
4	11.3	12.4	13.1	12.8	11.5	0.2	0.1	0.2	0.1	0.2
5	10.3	13.3	13.5	13.6	12.5	0.3	0.2	0.1	0.1	0.2
6	6.4	6.9	7.5	8.2	7.2	0.1	0.4	0.2	0.3	0.1
7	5.3	6.3	7.4	8.4	7.5	0.1	0.2	0.4	0.5	0.4

2.4.5.1 Comparison of Water Distribution Profiles

Figure 2.9 shows the application rate profiles of the newly designed dynamic fluidic sprinkler with different types of nozzles at 100, 150, 200 250 and 300 kPa, respectively. Generally, the application rates increased with an increase in nozzle diameters for all operating pressures, and these results are in agreement with [30]. As the distance from the sprinkler increased, the application rate also increased until it got to the maximum value and decreased for all the pressures. As operating pressure was increased, the application rates increased until they reached the maximum, when they started to decrease. The application rate of the 5.5-mm nozzle varied from 5.24 to 7.42 mm h − 1. The maximum value of the application rate was obtained for the five analyzed pressures (7.6 mm h − 1 at distances of 8 m for 100 kPa, 6.1 mm h − 1 at 10 m for 150 kPa, 6.23 mm h − 1 at 7 m for 200 kPa, 6.53 mm h − 1 at 7 m for 250 kPa and 7.42 mm h − 1 at 7 m for 300 kPa). Among the pressures, 200 kPa performed slight better than 150 kPa. The result from independent sample t-test analysis indicated that there was no significant difference between 250 and 150 kPa ($p > 0.05$). The comparison of the water distribution profiles at different operating pressures showed that all the different nozzle sizes produced parabola-shaped profiles, but the 5.5-mm nozzle size was flatter than the other nozzle sizes at a low pressure of 150 kPa. This could be attributed to the fact that flow rate at the same operating pressures was much higher and the internal turbulent flow was less uniform from the nozzle outlet, as well as more water was applied near the sprinkler, resulting in a more uniform water distribution for the 5.5-mm nozzle compared to the others. Several studies have shown that [37, 38] a doughnut-shaped water distribution leads to surface runoff because more water is deposited away from the sprinkler, affecting the quality of sprinkler irrigation. This implies that a 5.5-mm nozzle size can improve the non-uniform water distribution and save water for crop production. These results are better than those obtained by earlier researchers who used a similar sprinkler type.

Table 2.9 Independent sample *t*-test

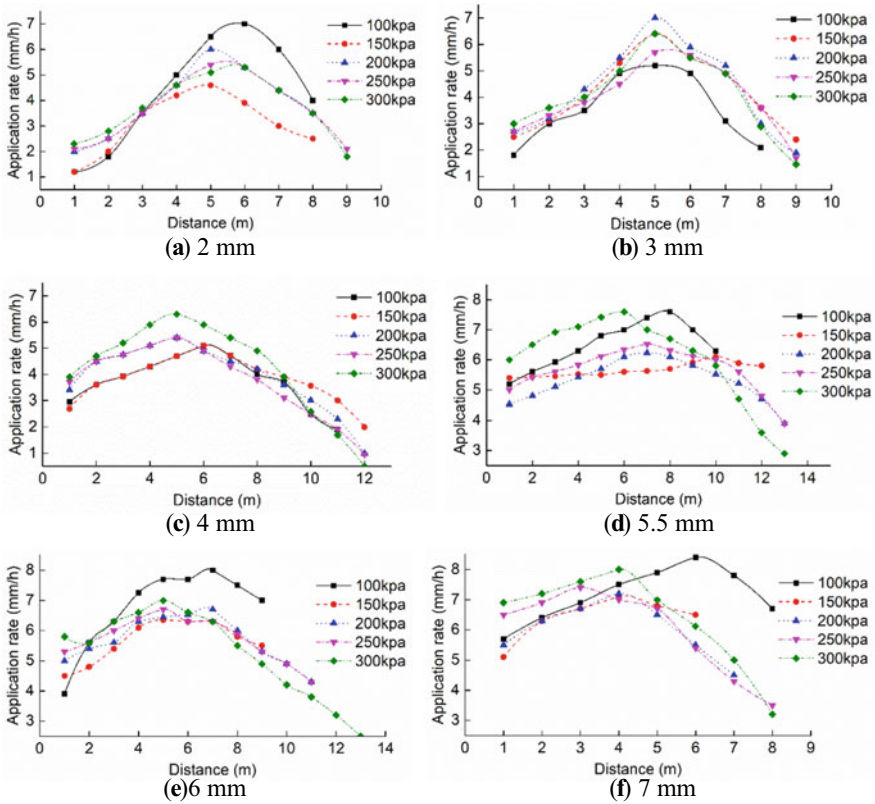|		Levene's test for equality of variances		*t*-Test for equality of means					95% Confidence interval of the difference	
		F	Sig	t	df	Sig. (2-tailed)	Mean difference	Std. error difference	Lower	Upper
Distance	Equal variances assumed	0.727	0.442	−2.530	4	0.065	−0.26667	0.10541	−0.55933	0.02600
	Equal variances not assumed			−2.530	3.448	0.075	−0.26667	0.10541	−0.57876	0.04542

Fig. 2.9 Water distribution profiles for different types of nozzles and pressures

2.4.5.2 Comparison of the Computed Uniformity Coefficient

Figure 2.10 presents the computed coefficients of uniformity with different types of nozzles at 100, 150, 200, 250 and 300 kPa, respectively. The computed coefficients of uniformity were determined using Eq. (1). The rectangular spacing for lateral radius times of 1.0, 1.1, 1.2, 1.3, 1.4, 1.5, 1.6, 1.7, 1.8, 1.9 and 2.0 was used for all the nozzle sizes in the study. Figure 2.6 shows the relationships between the simulated CU and spacing along the vertical and horizontal axis. As the distance from the sprinkler increased, the coefficient of uniformity also increased until it got to the maximum and then decreased for all the pressures and nozzles. The average of the computed values for the 5.5-mm nozzle size was (at different pressures) as follows; 76, 81, 77, 82 and 77% and 100, 150, 200, 250 and 300 kPa, respectively. Comparatively, 250 kPa performed slightly better than 150 kPa, but 150 kPa was selected as the optimum operating pressure because of rising energy costs. For all the nozzle sizes. 5.5 mm gave the highest computed uniformity value of 86%, at a low pressure of 150 kPa. This indicates that 5.5 mm produced a better water distribution pattern
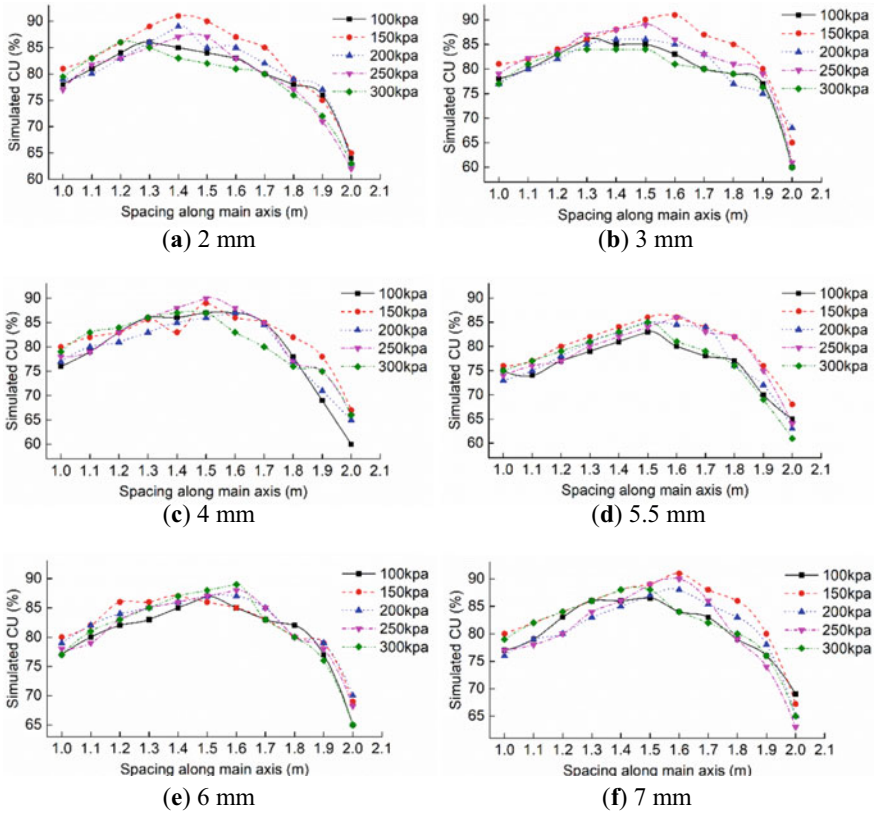
Fig. 2.10 Computed coefficient of uniformity (CU) for different types of nozzles and pressures

than the rest of the nozzles. These results are slightly better than those obtained by previous researchers for the complete fluidic sprinkler and the outside signals of 82 and 80.88%, respectively [27]. Although 250 kPa gave higher CU than 150, there was no significant difference ($p > 0.05$), along with the increasing cost of energy and growing demand for saving water for optimum crop production. It is appropriate to use 150 kPa.

The range of computed CU values for the 5.5-mm nozzle size at 150 kPa was as follows: 77% at a spacing of 1- to 68% at 2.0-times (150 kPa). The highest CU occurred at 1.6-times spacing uniformity and increased with a spacing of one- to 1.6-times, ranging from 76% to 86 with an average of 80%; subsequently, the uniformity decreased with spacing from 1.6- to 2.0-times; the CU value ranged from 84 to 68% with an average of 79.2% at an operating pressure of 150 kPa.

In general, CU values resulting from the 5.5-mm nozzle size were higher compared to other nozzles. The explanation could be that the internal turbulent flow was less uniform from the nozzle outlet and more water was applied near the sprinkler, resulting in a higher combined CU. This supports already established results

from earlier research works [24, 32, 39]. The performance of the tested sprinkler was better than earlier research for the different types of fluidic sprinklers.

2.4.5.3   Droplet Size Distributions

Figure 2.11 shows the cumulative droplet diameter frequency for different types of nozzles at different operating pressures. Low operating pressures resulted in larger droplet diameters, and as operating pressures increased, smaller droplets diameters were produced. Droplet diameter increased with distance from the sprinkler for the various nozzle sizes, which is similar to previous results obtained [40].

As can be seen in Fig. 2.11, 5.5 mm gave better results than the rest of the nozzles. The average droplet diameters ranged from 0 to 3.2 mm. The cumulative frequencies were under 1 mm of 87, 67, 86.73 and 99%, under 2 mm of 89, 77, 65, 67 and
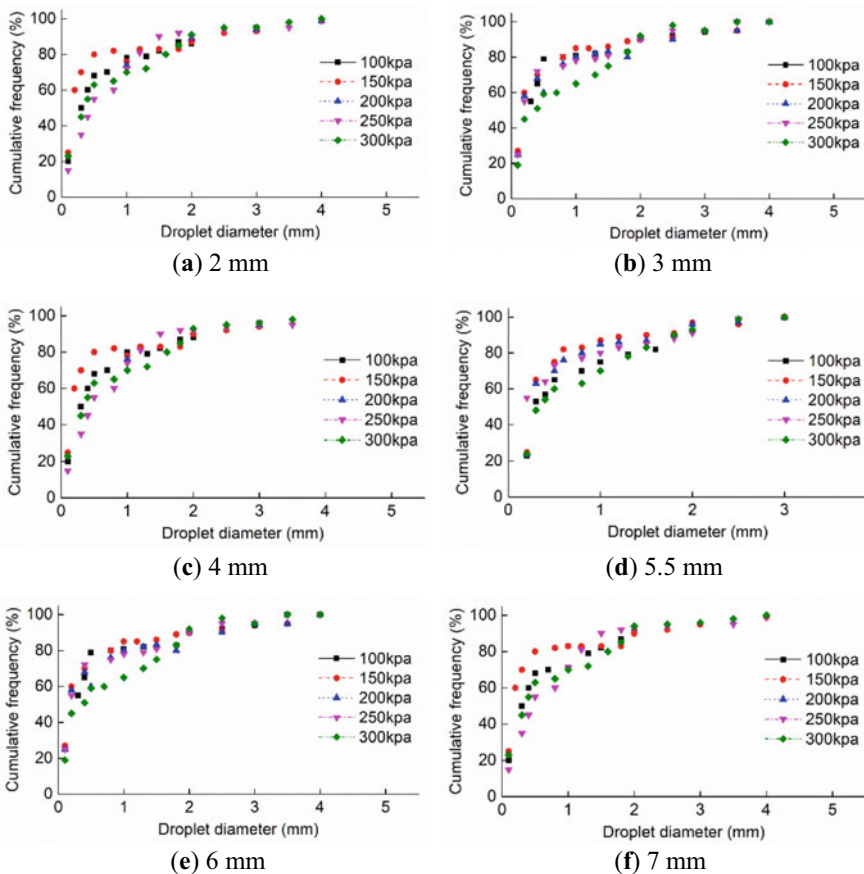

Fig. 2.11   Cumulative droplet diameter frequency

100% under 3 mm of 88, 90, 67, 88 and 55 at pressures of 100, 150, 200, 250 and 300 kPa, respectively. The mean droplet diameters for the nozzle sizes of 2, 3, 4, 5.5, 6 and 7 mm ranged from 0 to 4.2, 0 to 3.7, 0 to 3.6, 0 to 3.2,0 to 0.5 and 0 to 3.8 mm, respectively The comparison of droplet size distributions showed that 5.5 mm had the narrowest droplet size and smallest maximum droplet diameter of 3.2 mm. The biggest droplet size ranged with the maximum value of 4.2 for a nozzle size of 2 mm. These results are similar to those obtained by previous researchers who used different sprinkler types. It can also be noted that at most distances from the sprinkler, the number of droplets at smaller diameters was greater compared to that at larger diameters. This goes to support the hypothesis that droplet formation is a continuous process along the jet trajectory [41–43]. Using a 5.5-mm nozzle size will produce optimum droplet sizes, which can fight wind drift and evaporation losses. This is because large droplets possess high kinetic energy, and on impact, they disrupt the soil surface, especially soils with crustiness problems, leading to sealing of the soil surface. Dwomoah et al. reported similar results when analyzing drop diameter measurements performed with the Thies Clima Laser Precipitation Monitor (TCLPM).

Table 2.10 shows the percentage of droplets with a mean diameter for the various nozzle sizes at different operating pressures. Diameters d_{10}, d_{25}, d_{50}, d_{75} and d_{90} represent the diameters corresponding to 10, 25, 50, 75 and 90%, respectively, of the volume of detected water. From the table, it can be observed that for all the nozzle sizes, droplet size increased with increasing percentage of droplet diameter. In this experiment, almost 20% of the drops identified at all the distances from the sprinkler were smaller than the minimum diameter obtained from earlier researchers who used similar sprinkler types.

2.4.5.4   Droplet Characterization Statistics

Table 2.11 presents statistical parameters for the droplets for different types of nozzle at different operating pressures. Parameters include the arithmetic mean diameter, the volumetric mean diameter, the median diameter, the standard deviation and the coefficient of variation. All the parameters decreased with an increase in operating pressure for the nozzle sizes. All the parameters increased as the nozzle sizes increased for all the operating pressures. The mean droplet diameter and volumetric median diameter decreased with operating pressures for the nozzle sizes. Among the nozzles, 5.5 mm performed better than the rest of the nozzles. The standard deviation of the droplet diameter ranged from 0.69 to 0.86 with a mean of 0.775, and the coefficient of variation ranged from 91 to 147% with a mean value of 119% [33].

Table 2.10 Droplet sizes (mm) for 10, 25, 50, 75 and 90% ($d_{10}, d_{25}, d_{50}, d_{75}$ and d_{90}, respectively) for different types of nozzle

Nozzles size	Pressure (kPa)	d_{10}	d_{25}	d_{50}	d_{75}	d_{90}	Standard deviation (m)
2 mm	100	0.07	0.18	0.45	0.46	1.94	0.76
	150	0.05	0.14	0.36	1.09	1.55	0.65
	200	0.08	0.15	0.35	1.08	1.56	0.65
	250	0.07	0.16	0.27	1.09	1.85	0.7
	300	0.09	0.15	0.25	1.3	1.87	0.87
3 mm	100	0.06	0.13	0.36	0.47	2.09	0.83
	150	0.07	0.14	0.27	0.79	2.4	0.91
	200	0.06	0.15	0.25	0.82	2.3	0.93
	250	0.06	0.16	0.27	0.5	2.05	0.82
	300	0.09	0.18	0.25	1.49	1.96	0.87
4 mm	100	0.08	0.13	0.27	0.4	1.69	0.65
	150	0.07	0.15	0.26	0.71	1.88	0.75
	200	0.07	0.15	0.26	0.73	1.86	0.74
	250	0.08	0.17	0.26	1.02	1.82	0.74
	300	0.09	0.6	0.25	1.18	1.7	0.65
5.5 mm	100	0.04	0.11	0.34	0.44	2.05	0.69
	150	0.04	0.12	0.24	0.77	2.1	0.76
	200	0.04	0.12	0.23	0.79	2.1	0.75
	250	0.04	0.13	0.23	0.48	2.02	0.76
	300	0.05	0.14	0.23	0.47	1.93	0.70
6 mm	100	0.04	0.11	0.34	0.44	2.05	0.83
	150	0.05	0.12	0.24	0.77	2.1	0.85
	200	0.05	0.13	0.23	0.79	2.1	0.85
	250	0.05	0.14	0.23	0.48	2.02	0.81
	300	0.07	0.14	0.23	1.47	1.93	0.87
7 mm	100	0.05	0.16	0.44	0.44	1.92	0.76
	150	0.05	0.12	0.34	1.07	1.53	0.65
	200	0.07	0.13	0.33	1.06	1.51	0.63
	250	0.06	0.14	0.25	1.07	1.82	0.76
	300	0.06	0.13	0.23	1.28	1.84	0.80

d_{10} = represents 10% of the cumulative droplet frequency; d_{25} = represents 25% of the cumulative droplet frequency; d_{50} = represents the mean cumulative droplet frequency; d_{75} = represents 75% of the cumulative droplet frequency; d_{90} = represents 90% of the cumulative droplet frequency

Table 2.11 Droplet statistical parameter for droplet diameters for different types of nozzles

Nozzle size (mm)	Pressure (kPa)	$\bar{d}$	d_v	d_{50}	SD_D (m)	CV_D
2	100	0.73	3.12	0.45	0.94	119
	150	0.71	2.94	0.36	0.71	87
	200	0.70	2.79	0.35	0.81	107
	250	0.68	2.68	0.37	0.82	124
3	100	0.67	2.71	0.36	0.85	116
	150	0.69	2.09	0.27	0.71	125
	200	0.60	1.93	0.25	8.0	120
	250	0.59	1.68	0.23	0.84	114
4	100	0.78	2.81	0.27	0.84	107
	150	0.76	2.44	0.26	0.68	91
	200	0.73	2.0	0.26	0.71	99
	250	0.72	1.91	0.25	0.79	120
5	100	0.86	2.81	0.34	0.89	106
	150	0.77	2.34	0.24	0.68	91
	200	0.69	2.25	0.23	0.77	114
	250	0.57	2.20	0.21	0.83	147
6	100	0.89	2.80	0.37	1.02	115
	150	0.76	2.79	0.24	0.99	132
	200	0.70	2.19	0.23	0.95	136
	250	0.68	1.49	0.23	0.87	127
7	100	0.80	2.99	0.44	0.92	119
	150	0.79	2.39	0.35	0.67	85
	200	0.75	2.21	0.33	0.71	106
	250	0.66	1.92	0.25	0.79	121

$\bar{d}$ = arithmetic mean droplet; d_v = the volume weighted average droplet diameter; SD_D = the standard deviation; CV_D = is the coefficient of variation

2.4.6 Conclusion

This study evaluated the hydraulic performance of a newly designed dynamic fluidic sprinkler using different types of nozzles at different operating pressures. The following conclusions can be drawn.

The smallest radius of throw was obtained when the sprinkler was operated at the pressure of 100 kPa, while the maximum radius of throw was obtained when the sprinkler was operated at the pressure of 250 kPa. The distance of throw increased with the increase in diameters of nozzle sizes. However, there was no significant different between the radius of throw for 250 and 150 kPa. With the rising cost of energy, it is appropriate to operate under 150 kPa in order to save water.

The comparison of water distribution profiles at different operating pressures showed that all the different nozzle sizes produced parabola-shaped profiles, while the 5.5-mm nozzle size was flatter at a low pressure of 150 kPa. This implies that a 5.5-mm nozzle size can improve the non-uniform water distribution and save water for sprinkler-irrigated fields.

For all the nozzle sizes, 5.5 mm gave the highest computed uniformity value of 86%, at a low pressure of 150 kPa. There was no significant difference between 250 and 150 kPa. Comparatively, the sprinkler with a 5.5-mm nozzle produced a better uniformity, and the average CU obtained was within the acceptable range.

The mean droplet diameter for the nozzles sizes of 2, 3, 4, 5.5, 6 and 7 mm ranged from 0 to 4.2, 0 to 3.7, 0 to 3.6, 0 to 3.2, 0 to 0.5 and 0 to 3.8 mm, respectively. The comparison of the droplet size distribution for the various sizes showed that 5.5 mm had the optimum droplet diameter of 3.2 mm. The largest droplet size had a maximum value of 4.0 for a 2-mm nozzle size. Hence, using a 5.5 mm nozzle size can produce the optimum droplet sizes, which can minimize losses caused by wind drift and evaporation.

References

1. Kahlown MA, Raoof A, Zubair M, Kemper WD (2007) Water use efficiency and economic feasibility of growing rice and wheat with sprinkler irrigation in the Indus Basin of Pakistan. Agric Water Manag 87:292–298
2. Montazar A, Sadeghi M (2008) Effects of applied water and sprinkler uniformity on alfalfa growth and hay yield. Agric Water Manag 95:1279–1287
3. Kincaid DC (1996) Spray drop kinetic energy from irrigation sprinklers. Trans ASAF 39:847–853
4. Kulkarni S (2011) Innovative technologies for Water saving in Irrigated Agriculture. Int J Water Resour Arid Environ 1:226–231
5. Howell TA (2001) Enhancing water use efficiency in irrigated agriculture. Agronomy J 93:281–289
6. Shin S, Bae S (2013) Simulation of water entry of an elastic wedge using the FDS scheme and HCIB method. J Hydrodynamics 25:450–458
7. Darko RO, Yuan SQ, Liu JP, Yan HF, Zhu XY (2017) Overview of advances in improving uniformity and water use efficiency of sprinkler irrigation. Int J Agric Biol Eng 10:1–15
8. Liu JP, Zhu XY, Yuan SQ, Wan JH, Chikangaise P (2018) Hydraulic performance assessment of sprinkler irrigation with rotating spray plate sprinklers in indoor experiments. J Irrig Drain Eng 144. https://doi.org/10.1061/(ASCE)IR.1943-4774.0001333
9. Li J, Rao M (2000) Sprinkler water distributions as affected by winter wheat canopy. Irrig Sci 20:29–35
10. Tang LD, Yuan SQ, Qiu ZP (2018) Development and research status of water turbine for hose reel irrigator. J Drain Irrig Mach Eng 36:963–968
11. Al-Ghobari HM (2006) Effect of maintenance on the performance of sprinkler irrigation systems and irrigation water conservation. Food Sci Agric Res Cent Res Bull 141:1–6
12. Kohl RA, Koh KS, Deboer DW (1987) Chemigation drift and volatilization potential. Appl Eng Agric 3:174–177
13. Dwomoh FA, Yuan SQ, Li H (2014) Sprinkler rotation and water application rate for the newly designed complete fluidic sprinkler and impact sprinkler. Int J Agric Biol Eng 7:38–46

14. Zhu X, Chikangaise P, Shi W, Chen WH, Yuan S (2018) Review of intelligent sprinkler irrigation technologies for remote autonomous system. Int J Agric Biol Eng 11:23–30
15. DeBoer DW, Monnens MJ, Kincaid DC (2001) Measurement of sprinkler drop size. Appl Eng Agric 17:11–15
16. Kohl RA, Bernuth RD, Heubner G (1985) Drop size distribution measurement problems using a laser unit. Trans ASAE 28:190–192
17. Fukui Y, Nakanishi k, Okamura S (1980) Computer elevation of sprinkler uniformity. Irrig Sci 2:23–32
18. Thompson A, Gilley JR, Norman JM (1993) Sprinkler water droplet evaporation a plant canopy model. Trans ASARE 36:743–750
19. Lorenzini G, Wrachien D (2005) Performance assessment of sprinkler irrigation system a new indicator for spray evaporation losses. J Int Commun Irrig Drain 54:295–305
20. Bautista C, Salvador R, Burguete J (2009) Comparing methodologies for the characterization of water drops emitted by an irrigation sprinkler. Trans ASABE 52:1493–1504
21. Wilcox JC, Swailes GE (1947) Uniformity of water distribution by some under tree orchard sprinklers. Sci Agric 27:565–583
22. Hart WE, Reynolds WN (1965) Analytical design of sprinkler systems. Trans Am Soc Agric Eng 8:83–85
23. Kay M (1988) Sprinkler irrigation equipment and practice; Batsford Limited. London, UK
24. Keller J, Bliesner RD (1990) Sprinkle and trickle irrigation; Van Nostrand Reinhold Pun. New York, NY, USA
25. Xiang QJ, Xu ZD, Chen C (2018) Experiments on air and water suction capability of 30PY impact sprinkler. J Drain Irrig Mach Eng 36:82–87
26. Karmeli D (1978) Estimating sprinkler distribution pattern using linear regression. Trans ASAE 21:682–686
27. Liu JP, Liu WZ, Bao Y, Zhang Q, Liu XF (2017) Drop size distribution experiments of gas-liquid two phase's fluidic sprinkler. J Drain Irrig Mach Eng 35:731–736
28. Liu JP, Yuan SQ, Li H, Zhu XY (2013) Numerical simulation and experimental study on a new type variable-rate fluidic sprinkler. J Agric Sci Technol 15:569–581
29. Dwomoh FA, Yuan S, Hong L (2013) Field performance characteristics of fluidic sprinkler. Appl Eng Agric 29:529–536
30. Zhu X, Yuan S, Jiang J, Liu J, Liu X (2015) Comparison of fluidic and impact sprinklers based on hydraulic performance. Irrig Sci 33:367–374
31. Zhang AM, Sun PN, Ming FR, Colagrossi A (2017) Smoothed particle hydrodynamics and its applications in fluid-structure interactions. J Hydrodynamics 29:187–216
32. Zhu X, Yuan S, Liu J (2012) Effect of sprinkler head geometrical parameters on hydraulic performance of fluidic sprinkler. J Irrig Drain Eng 138:1019–1026
33. Zhu X, Fordjour A, Yuan S, Dwomoh F, Ye D (2018) Evaluation of hydraulic performance characteristics of a newly designed dynamic fluidic sprinkler. Water 10(10):1301. https://doi.org/10.3390/w10101301
34. Coanda H (1936) Device for deflecting a stream of elastic fluid projected into an elastic fluid. U.S. Patent No. 2,052,869, 1 Spetember 1936
35. American Society of Biological Enginees (1985) Procedure for sprinkler testing and performance reporting. ASAE S398.1: St. Joseph MI, United States
36. Al-araki GY (2002) Design and evaluation of sprinkler irrigation system. Doctoral Dissertation; University of Khartoum: Khartoum, Sudan
37. Chen D, Wallender WW (1985) Droplet size distribution and water application with low-pressure sprinklers. Trans ASAE 28:511–516
38. Li J, Kawano H, Yu K (1994) Droplet size distributions from different shaped sprinkler nozzles. Trans ASAE 37:1871–1878
39. Tarjuelo JM, Montero J, Valiente M, Honrubia FT, Ortiz J (1999) Irrigation uniformity with medium size sprinkler, part I: characterization of water distribution in no—wind conditions. Trans ASAE 42:677–689

40. King BA, Winward TW, Bjorneberg DL (2013) Comparison of sprinkler droplet size and velocity measurements using a laser precipitation meter and photographic method. Am Soc Agric Biol Eng 131594348. https://doi.org/10.13031/aim.20131594348
41. Sudheera KP, Panda RK (2000) Digital image processing for determining drop sizes from irrigation spray nozzles. Agric Water Manag 45:159–167
42. Liu J, Liu X, Zhu X, Yuan S (2016) Droplet characterization of a complete fluidic sprinkler with different nozzle dimensions. Biosyst Eng 148:90–100
43. Lu J, Cheng J (2018) Numerical simulation analysis of energy conversion in hydraulic turbine of hose reel irrigator JP75. J Drain Irrig Mach Eng 36:448–453